Azaferrocenophanes with Azobenzene-Containing Ligands − Protonation and Electrochemical Oxidation of the Molecule Influences the Absorption Spectra and *cis*−*trans* Isomerization of the Azobenzene Group

Tatsuaki Sakano,[a] Masaki Horie,[a] Kohtaro Osakada,*[a] and Hidenobu Nakao[b]

Keywords: Azobenzene / Chromophores / Ferrocene / Photochemistry / Redox chemistry

N-{4-(Phenylazo)phenyl}aminophenyl-2-aza-[3]-ferrocenophane (**4**) and *N*-{3-(phenylazo)phenyl}aminophenyl-2-aza-[3]-ferrocenophane (**5**) have been prepared by C–N bond-forming reactions catalyzed by Ru and Pd complexes. The absorption peaks due to the π–π^* transition of the *trans*-azobenzene group of **4** and **5** appear at 442 and 426 nm, respectively, in toluene. Photoirradiation of solutions of **4** and **5** at 420 nm causes partial isomerization of the *trans*-azobenzene group to *cis*-azobenzene and reaches a photostationary state. The compounds at the photostationary state undergo thermal isomerization of the *cis*-azobenzene group to the *trans* isomer. The isomerization after one-electron oxidation of the compounds takes place more rapidly than that without electrochemical oxidation.

Introduction

Several organometallic compounds have potential utility as materials for opto-electronic devices which exhibit electroluminescence, liquid-crystalline properties, and perform as biosensors.[1] The introduction of functional groups to the cyclopentadienyl ligands of ferrocene forms ferrocene derivatives, which can be utilized as a mediator and electron donor in electrochemical reactions and electron-transfer systems.[2] Since azobenzene changes its molecular shape and the absorption peak positions upon photoirradiation or heating,[3] binding the ferrocene and azobenzene with a suitable linker would provide compounds where the electrochemical properties of the Fe center and the optical response of the organic group are linked to each other.[4] Nishihara has reported the unique properties of *m*-ferrocenylazobenzene, in which azobenzene is directly bonded to a cyclopentadienyl ligand.[5] One-electron oxidation of the compound led to the formation of a *trans*-rich mixture in the Fe^{III} state upon irradiation with a single green light, while it was converted to a *cis*-rich mixture upon electrochemical reduction to Fe^{II}.

Recently we have prepared ferrocene derivatives with an aminomethyl substituent at the cyclopentadienyl ligand and found electrochemical communication between the ferrocene and the organic group of the ligand by electron transfer between the Fe center and the N atom.[6] N-Substituted 2-aza-[3]-ferrocenophanes also undergo similar electron transfer between the metal center and the organic group of the ligand.[7,8] These compounds may show cooperative responses to a photo- or electrochemical stimulus. In this paper we report the preparation of new 2-aza-[3]-ferrocenophanes containing azobenzene in the ligand, as well as their molecular structures and their absorption spectra, which change upon protonation and electrochemical oxidation. Part of this work has been reported in a preliminary form.[9]

[a] Chemical Resources Laboratory, Tokyo Institute of Technology, 4259 Nagatsuta, Midori-ku, Yokohama, 226-8503 Japan
Fax: (internat.) + 81-45-924-5224
E-mail: kosakada@res.titech.ac.jp
[b] Instrumentational Engineering Laboratory, National Food Research Institute, 2-1-12 Kannodai, Tsukuba, 305-8642 Japan

Results and Discussions

Preparation and Characterization

The synthesis of the new ferrocenophanes with an azobenzene group is summarized in Scheme 1. Dehydrative condensation of 1,1′-ferrocenedimethanol with 4-aminoazobenzene catalyzed by $[RuCl_2(PPh_3)_3]$[10] produces *N*-{4-(phenylazo)phenyl}-2-aza-[3]-ferrocenophane (**1**). Similar reactions with 4-bromoaniline and with 3-bromoaniline form *N*-(4-bromophenyl)-2-aza-[3]-ferrocenophane (**2**) and *N*-(3-bromophenyl)-2-aza-[3]-ferrocenophane (**3**), respectively. The ferrocenophanes react with 4-(phenylamino)azobenzene in the presence of $Pd_2(dba)_3$/P*t*Bu$_3$ [dba = di-(benzylidene)acetone] catalyst and NaO*t*Bu to afford *N*-{4-(phenylazo)phenyl}-2-aza-[3]-ferrocenophane (**4**) and *N*-{3-(phenylazo)phenyl}-2-aza-[3]-ferrocenophane (**5**), respectively. Analogous Pd-catalyzed cross-coupling reactions of bromoarene with secondary amines have been reported to form a new C−N bond.[11−13]

  DOI: 10.1002/ejic.200400592

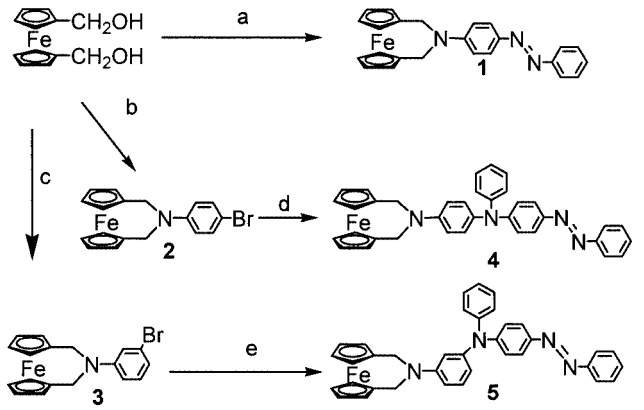

Scheme 1. (a) 4-phenylazoaniline (1 equiv.), $[RuCl_2(PPh_3)_3]$ (5 mol %), 180 °C, NMP; (b) 4-bromoaniline (1 equiv.), $[RuCl_2(PPh_3)_3]$ (5 mol %), 180 °C, NMP; (c) 3-bromoaniline (1 equiv.), $[RuCl_2(PPh_3)_3]$ (5 mol %), 180 °C, NMP; (d) 4-phenylazodiphenylamine (1 equiv.), $[Pd_2(dba)_3]$ (1.3 mol %), NaO*t*Bu (1.5 equiv.), P(*t*Bu)$_3$ (7.5 mol %), 100 °C, toluene

The ferrocenophanes with azobenzene-containing ligands (**1**, **4**, and **5**) were characterized by NMR spectroscopy and X-ray crystallography. Figure 1 depicts the molecular structures of **1**, **4**, and **5**, as determined by X-ray crystallography. The two cyclopentadienyl ligands have a staggered conformation, similar to other structurally characterized [3]-ferrocenophanes.[8,9] The diazene moiety (N=N bond) in the compounds has a *trans* conformation [N=N bond lengths: **1**: 1.276(7) Å; **4**: 1.232(7) and 1.197(7) Å; **5**: 1.227(5) Å; C−N=N bond angles: **1**: 113.3(6) and 116.2(6)°; **4**: 113.0(6), 110.4(6), 109.7(6), and 109.1(6)°; **5**: 112.1(5) and 113.2(5)°]. The N−C(phenyl) bond in the ferrocenophane ring [**1**: 1.355(8) Å; **4**: 1.393(8) and 1.398(8) Å; **5**: 1.384(4) Å] is shorter than the N−CH_2 bond (1.45−1.48 Å), which suggests a partial double-bond character of the former.[14]

Absorption Spectra and trans−cis Isomerization

Figure 2 shows the absorption spectra of **1**, **4**, and **5**. These complexes have peaks due to the π−π* transition of the *trans*-azobenzene group at 413 nm (**1**; ε = 19900 $M^{-1}\cdot cm^{-1}$), 442 nm (**4**; ε = 28000 $M^{-1}\cdot cm^{-1}$), and 426 nm (**5**; ε = 31500 $M^{-1}\cdot cm^{-1}$). The order of wavelengths of the π−π* transition, **4** > **5** > **1**, can be attributed to different degrees of π-conjugation of the azobenzene-containing ligands. Compound **4**, with a *p*-diaminophenylene group bonded to the phenylaminoazobenzene group, has the absorption peak at longer wavelength than **1**, without a diaminophenylene group, and **5**, with a *m*-diaminophenylene group.

The *trans*-azobenzene group of **4** undergoes partial isomerization to the *cis* form upon irradiation at 420 nm (Xenon lamp). Figure 3a shows change of the absorption spectra during the reaction at 25 °C in toluene. The peak intensity of the π−π* band of the *trans*-azobenzene group of **4** decreases in intensity and is accompanied by a shift of the peak to 457 nm. The new minor absorption is assigned to the n−π* transition of the *cis*-azobenzene group formed by photo-induced isomerization. The intensity of the ab-

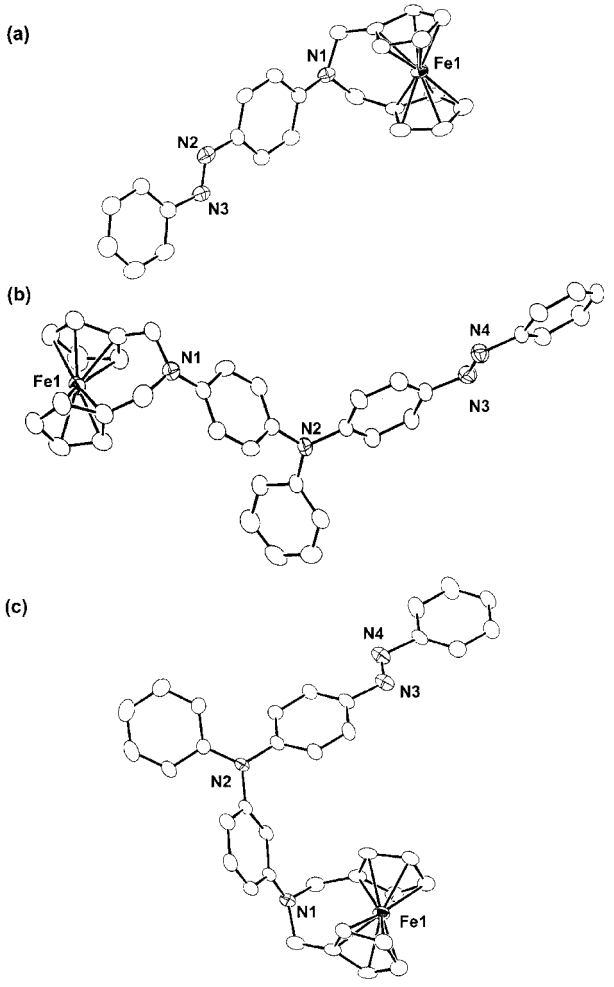

Figure 1. (a) An ORTEP drawing of **1**; selected bond lengths (Å) and angles (°): C1−C11 1.497(9), C6−C12 1.500(9) N1−C11 1.467(7), N1−C12 1.484(8), N1−C13 1.355(8), N2−C16 1.402(8), N2−C19 1.436(8), N2−N3 1.276(7); C11−N1−C12 112.9(5), C11−N1−C13 122.9(5), C12−N1−C13 121.8(6), N1−C11−C1 114.5(5), N1−C12−C6 114.4(5), N2−C16−C15 116.9(6), N2−C16−C17 125.0(6), N2−N3−C19 113.3(6), N3−N2−C16 116.2(6), N3−C19−C20 123.8(7), N3−C19−C24 115.6(7); (b) An ORTEP drawing of **4**; only one of the crystallographically independent molecules is shown; selected bond lengths (Å) and angles (°): C1−C11 1.52(1), C6−C12 1.51(1) N1−C11 1.44(1), N1−C12 1.46(1), N1−C13 1.393(8), N2−C16 1.433(8), N2−C19 1.410(8), N2−C25 1.429(8), N3−C28 1.456(8), N4−C31 1.470(8), N3−N4 1.232(7); C11−N1−C12 113.1(6), C11−N1−C13 121.3(7), C12−N1−C13 120.6 (6), C16−N2−C19 118.5(6), C16−N2−C25 121.7(6), C19−N2−C25 119.6(6), N1−C11−C1 114.6(6), N1−C12−C6 116.1(6), N1−C13−C14 121.3(8), N1−C13−C18 122.8(5), N2−C16−C15 120.4(7), N2−C16−C17 120.4(7), N2−C19−C20 119.3(7), N2−C19−C24 122.3(7), N2−C25−C26 119.2(6), N2−C25−C30 121.0(6), N3−C28−C27 124.1(6), N3−C28−C29 116.0(6), N3−N4−C28 113.0(6), N3−N4−C31 110.4(6), N4−N3−C28 113.0(6), N4−N3−C31 110.4(6), N4−C31−C32 114.1(6), N4−C31−C36 125.5(6); (c) An ORTEP drawing of **5**; selected bond lengths (Å) and angles (°): C1−C11 1.512(7), C6−C12 1.497(7) N1−C11 1.458(6), N1−C12 1.467(6), N1−C13 1.384(6), N2−C15 1.441(6), N2−C19 1.401(6), N2−C25 1.424(6), N3−C28 1.441(6), N4−C31 1.463(7), N3−N4 1.227(5); C11−N1−C12 113.4(5), C11−N1−C13 120.2(4), C12−N1−C13 120.5 (4), C15−N2−C19 119.1(4), C15−N2−C25 119.1(4), C19−N2−C25 121.7(4), N1−C11−C1 113.8(4), N1−C12−C6 115.0(4), N1−C13−C14 121.3(8), N1−C13−C18 122.8(5), N2−C15−C14 118.8(5), N2−C15−C16 119.3(5), N2−C19−C20 120.4(5), N2−C19−C24 121.2(5), N2−C25−C26 120.5(6), N2−C25−C30 120.7(5), N3−C28−C27 114.5(6), N3−C28−C29 125.6(5), N3−N4−C31 113.2(5), N4−N3−C28 112.1(5), N4−C31−C32 125.1(6), N4−C31−C36 114.0(6)

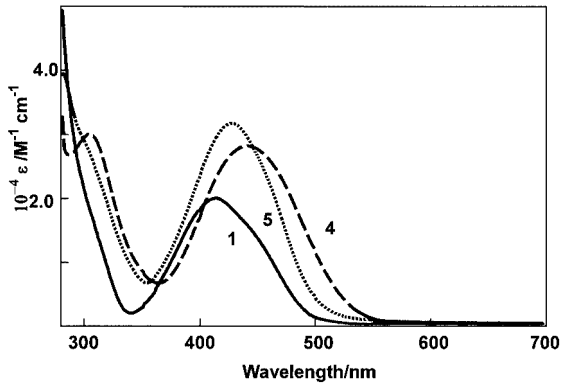

Figure 2. Absorption spectra of **1** (2.5×10^{-5} M in $CHCl_3$, solid line), **4** (2.5×10^{-5} M in toluene, dashed line), and **5** (2.5×10^{-5} M in toluene, dotted line) at 25 °C; wavelength at maximum absorbance and absorption coefficients are determined as: λ_{max} = 413 nm and ε = 19900 $M^{-1}\cdot cm^{-1}$ (**1**); λ_{max} = 442 nm and ε = 28000 $M^{-1}\cdot cm^{-1}$ (**4**); λ_{max} = 426 nm and ε = 31500 $M^{-1}\cdot cm^{-1}$ (**5**)

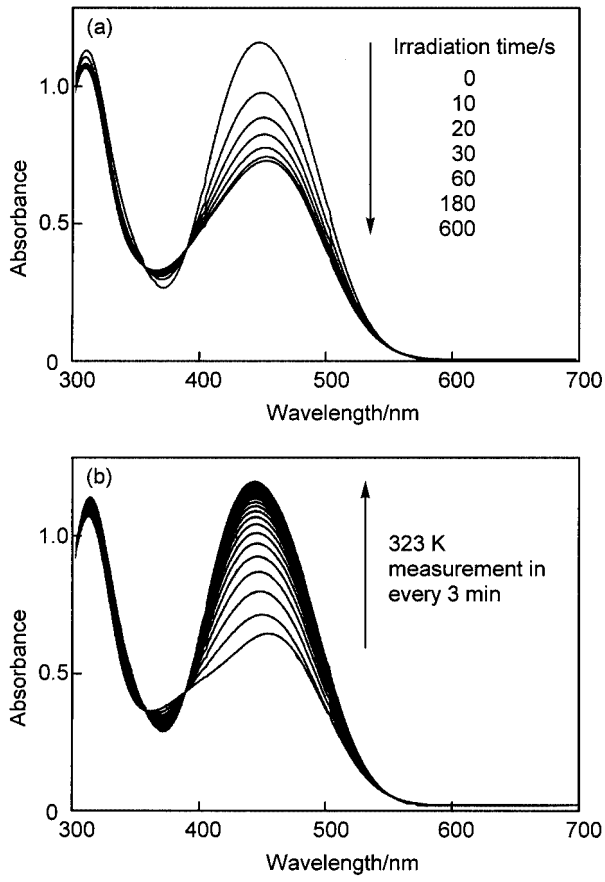

Figure 3. Change of the absorption spectrum of **4** caused by (a) photoisomerization with irradiation at 420 nm at 25 °C in toluene, and (b) thermal isomerization of the photostationary state at 50 °C in toluene

sorbance at 442 nm decreases to 41% of the original spectrum of **4**.

Heating the solution of **4** at the photostationary state in the dark at 50 °C causes growth of the π−π* band of *trans*-azobenzene group (Figure 3b). Recovery of the absorbance of **4** with all the azobenzene groups *trans* takes 30 min at this temperature. The spectra taken during the photo-induced isomerization of the *trans*-azobenzene group to *cis* the structure and thermal isomerization in the reverse direction contain isosbestic points at 335 nm and 387 nm, respectively. Table 1 summarizes the kinetic data of the thermal isomerization of **4** monitored by the increase of the absorbance at 430 nm at 30−70 °C. The reaction obeys first-order kinetics with respect to the concentration of the *cis*-azobenzene group. The reaction enthalpies are estimated to be 9.5 kcal·mol^{-1} in toluene and 7.9 kcal mol^{-1} in MeCN. Compound **5** also undergoes photochemical isomerization of the *trans*-azobenzene group to the *cis* form and thermally induced isomerization of the *cis*-azobenzene group to the *trans* form. The reaction enthalpies of the latter reaction were determined to be 13.5 kcal mol^{-1} and 7.0 kcal mol^{-1} in toluene and in MeCN, respectively. The rate constants of the reaction in toluene are larger than those in MeCN.

Table 1. Kinetic data of the thermally induced *cis*-to-*trans* isomerization

	Solvent	10^3 k_{obs} (s^{-1})			$\Delta H^{\ddagger}$ (kcal mol^{-1})
		323 K	333 K	343 K	
4	toluene	1.02	2.63	5.99	9.5
4	MeCN	0.83	1.93	3.81	7.9
5	toluene	4.01	5.30	10.3	13.5
5	MeCN	0.48	0.92	1.88	7.0

Protonation of 1 and 4

Addition of CF_3COOH to $CHCl_3$ solutions of **1** and **4** with *trans*-azobenzene groups causes a significant change of the spectra, as shown in Figure 4. Addition of CF_3COOH to the solution of **1** causes a decrease in the intensity of the π−π* transition peak at 398 nm and the growth of a new peak at 550 nm (Figure 4a). An isosbestic point at 460 nm is observed throughout the reaction. The new peak can be assigned to a diazaquinoid structure by comparison of the peak position with those of oxidized species of polyaniline and *p*-bis(dimethylamino)benzene.[15] Protonation of 4-(phenylamino)azobenzene with CF_3COOH also results in a decrease of the intensity of the initial peak at 400 nm and the growth of a new peak at 541 nm. Scheme 2 shows a plausible pathway to account for the change of the spectra. Initial protonation takes place either at the nitrogen of the ferrocenophane or the nitrogen of azobenzene. The two species formed can be transformed reversibly into each other by proton transfer. The species protonated at the azobenzene nitrogen is stabilized by a contribution from structure **A**, with a diazaquinoid group. The absorption of the protonated compound at 550 nm is attributed to structure **A**.

Protonation of compound **4** occurs in a stepwise manner, as shown in Figure 4b. Initial addition of CF_3COOH causes a shift of the peak at 450 nm to 405 nm, which is a similar position to **1**. Further addition of CF_3COOH causes a decrease of the intensity of the peak at 405 nm with concomi-

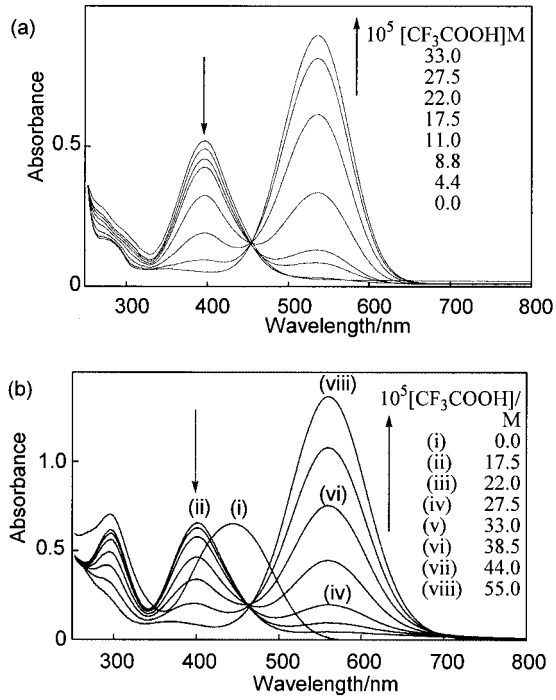

Figure 4. Change in the absorption spectra of (a) **1** (2.5×10^{-5} M in $CHCl_3$) and (b) **4** (2.5×10^{-5} M in $CHCl_3$) upon addition of CF_3COOH

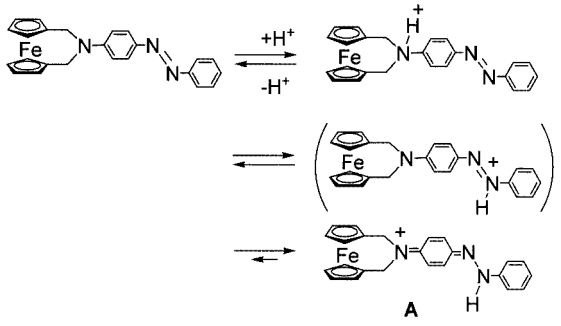

Scheme 2

tant growth of a peak at 570 nm with an isosbestic point at 472 nm. A plausible mechanism for the stepwise protonation of **4** is summarized in Scheme 3.

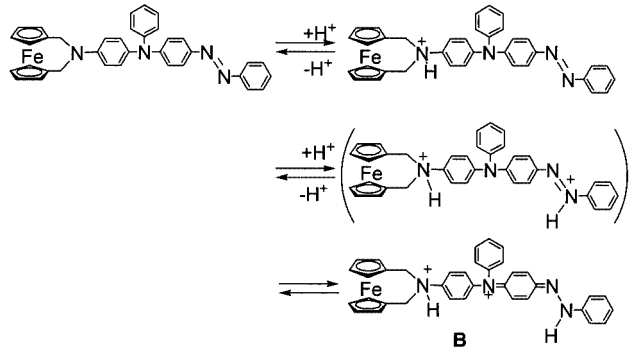

Scheme 3

Initial protonation occurs at the nitrogen atom in the ferrocenophane ring, which restricts π-conjugation of the *p*-diaminophenyelene group and causes a shift of the π−π* transition peak to a higher energy level. Further protonation of the azobenzene nitrogen causes formation of a tautomeric dication **B**. A resonance structure with a diazaquinoid group in the ligand serves to generate a π-conjugated system which shows an intense π−π* absorption at 570 nm.

Electrochemical Oxidation

Previously we have reported the electrochemical oxidation of various 2-aza-[3]-ferrocenophane derivatives.[7,8] The compounds with 4-hydroxyphenyl and with 4-aminophenyl substituents at the nitrogen atoms exhibit three reversible cycles of oxidation and reduction in the cyclic voltammograms, while those with phenyl or alkyl substituents undergo one reversible and one irreversible oxidation reaction. These results suggest a different structure for the product of the second oxidation, as shown in Scheme 4. The ferrocenium species formed upon initial oxidation of the Fe center is in equilibrium with the Fe^{II} species having a cation radical at the nitrogen within the ferrocenophane ring. The cation radical formed in Scheme 4(i) undergoes further electrochemical oxidation to produce the stable quinodiimine. The formed cation radical would release both a proton and an electron under the oxidation conditions to form an iminium-containing product. Similar electron transfer between an Fe center and an amino group, followed by irreversible reaction has been discussed previously for the electrochemical oxidation of ferrocenophanes containing pendant amino groups.[7]

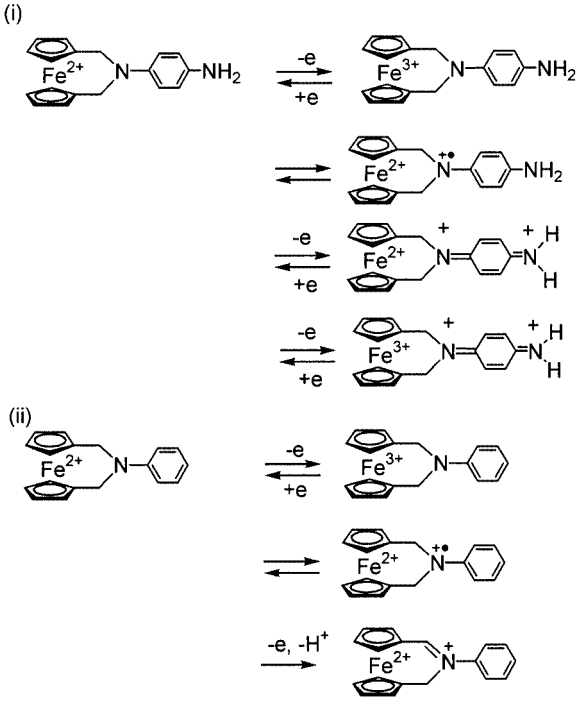

Scheme 4

The cyclic voltammograms of **1**, **4**, and **5** in CH_2Cl_2 are shown in Figure 5. Compound **1** undergoes a reversible reduction at $E_{1/2}$ = +0.05 V and an irreversible oxidation at E_{pa} = +0.75 V. The former was assigned to the redox potential of the ferrocenophane group, based on a comparison of the reduction potential of ferrocene ($E_{1/2}$ = +0.08 V). The CV peak at +0.75 V is due to further electrochemical oxidation of the organic group in the molecule.[6,16] The cyclic voltammogram of **4** in CH_2Cl_2 solution (see b in Figure 5) exhibits three redox peaks at $E_{1/2}$ = +0.17, +0.41, and +0.92 V. The second electrochemical oxidation occurs more easily than the second oxidation of **1**. Scheme 5 summarizes a plausible mechanism for the total electrochemical reaction. The oxidation of the ferrocene group ($E_{1/2}$ = +0.17 V) leads to formation of the ferrocenium cation, which is in equilibrium with the species with Fe^{II} and a cation radical at the nitrogen atom. The second oxidation occurs easily at the nitrogen bonded to three benzene rings (+0.41 V) to afford the stable dicationic quinodiimine structure. Further reversible oxidation (+0.92 V) occurs at the Fe^{II} center of the product of the second oxidation to afford the dicationic Fe^{III} product.

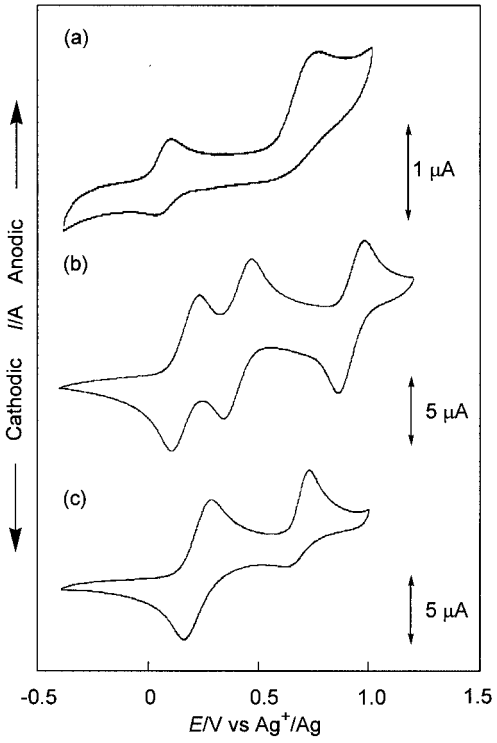

Figure 5. Cyclic voltammograms of (a) **1** (1.0 mM) in CH_2Cl_2 containing 0.10 M Et_4NBF_4 ($E_{1/2}$ = 0.05 V and E_{pa} = 0.75 V), (b) **4** (1.0 mM) in CH_2Cl_2 containing 0.10 M Et_4NBF_4 ($E_{1/2}$ = 0.17 V, 0.41 V, and 0.92 V), and (c) **5** (1.0 mM) in CH_2Cl_2 containing 0.10 M nBu_4NPF_6 ($E_{1/2}$ = 0.22 V and E_{pa} = 0.73 V); sweep rate: 0.10 V s^{-1}; measurement was carried out at 25 °C

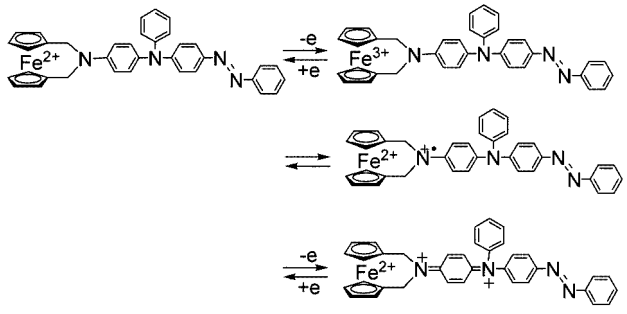

Scheme 5

The cyclic voltammogram of **5** contains a reversible redox peak at $E_{1/2}$ = +0.22 and a quasi-reversible oxidation peak at E_{pa} = +0.73 V. The second oxidation accompanies loss of a proton from the CH_2CN group to form a *meta*-azaquinoid structure.

Figure 6 (a) depicts the change of the absorption spectra during the electrochemical oxidation of **4** in a flow electrolysis cell. Spectrum (i) shows the absorption peak due to **4** (440 nm) exclusively. Spectra (ii) (obtained at −0.1 V) and (iii) (0.3 V) contain peaks at 440 nm and 770 nm, respectively. The latter peak is assigned to the radical cation in Scheme 5. The peak position suggest delocalization of the radical within the π-conjugated ligand. Spectrum (iv) (at 1.0 V) exhibits a new absorption band at 550 nm, which is ascribed to the species with a quinodiimine structure. The change of the absorbance at 440 nm, 550 nm, and 770 nm is shown in part b of Figure 6. It is consistent with the re-

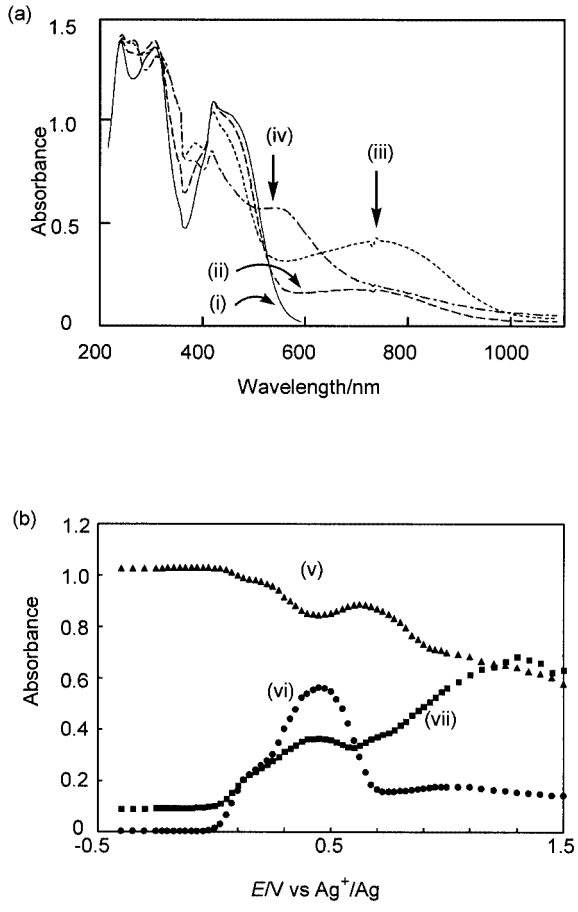

Figure 6. (a) Changes of absorption spectra of **4** (0.05 mM) in acetonitrile solution of 0.1 M Et_4NBF_4 at (i) −0.4 V, (ii) −0.1 V, (iii) 0.3 V, and (iv) 1.0 V (vs Ag^+/Ag); (b) relative intensity changes of absorption spectra of **4** induced by oxidation potentials (v) at 440 nm, (vi) at 550 nm, and (vii) at 770 nm

sults of CV (see b in Figure 5) and the proposed mechanism of the reaction shown in Scheme 5: the peaks at 770 nm and at 550 nm grow upon oxidation at −0.05−0.3 V and that at 0.3−0.4 V, respectively. Attempts to obtain clear ^{1}H NMR spectra of the oxidized species did not succeed due to significant broadening of the signals.

Electrochemical oxidation of **4** and **5**, both with the azobenzene group *trans*, at 0.30 and 0.40 V (vs Ag^+/Ag), causes little change in the positions of the π−π* transition peaks compared to those before electrolysis. Irradiation of the solutions at 420 nm after electrolysis causes a slight decrease of the peak intensity [approximately 5% (**4**) and 8% (**5**) of the original absorbance], as shown in Figure 7, which suggests that the photostationary states of the oxidized compounds contain *cis*-azobenzene as the minor components. The spectra returned rapidly to the original spectra containing the *trans*-azobenzene group. This can be ascribed to the higher stability of the *trans*-azobenzene group than the *cis*-azobenzene group even during photoirradiation, or faster, thermally induced isomerization of the *cis*-azobenzene group to the *trans* than the photo-assisted isomerization in the reverse direction. In order to obtain further insights, thermal isomerization of the *cis*-azobenzene obtained in the photostationary state of **4** and **5** was conducted after electrochemical oxidation.

Figure 8 compares the kinetic data of the thermal isomerization of the *cis*-azobenzene group to the *trans* form before and after electrolysis, which was monitored by the change in the absorbance at 430 nm. The rate of thermal isomerization actually increases with the electrochemical oxidation. The thermal isomerization was monitored by the spectroscopic change at 10 °C; it is complete within 5 min at this temperature.

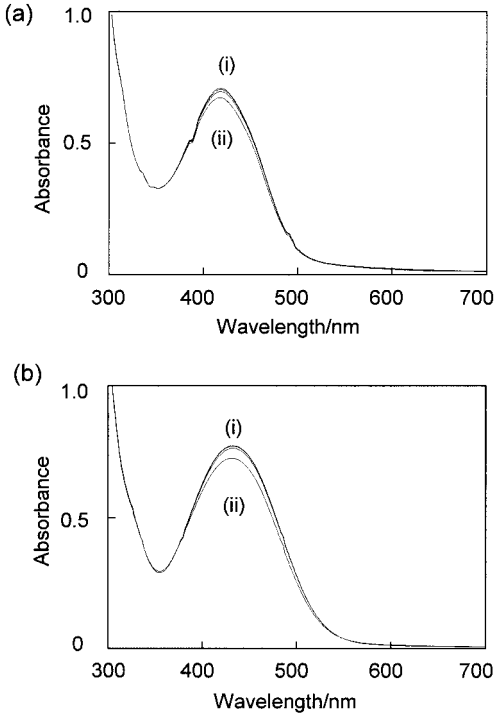

Figure 7. (a) Absorption spectra of **4** (i) before and (ii) after irradiation at 420 nm from a cut-off filtered Xenon lamp for 1 h at 20 °C in toluene; (b) absorption spectra of **5** (i) before and (ii) after irradiation; the data were obtained by flow-electrolysis at 0.3 V (a) and at 0.4 V (b)

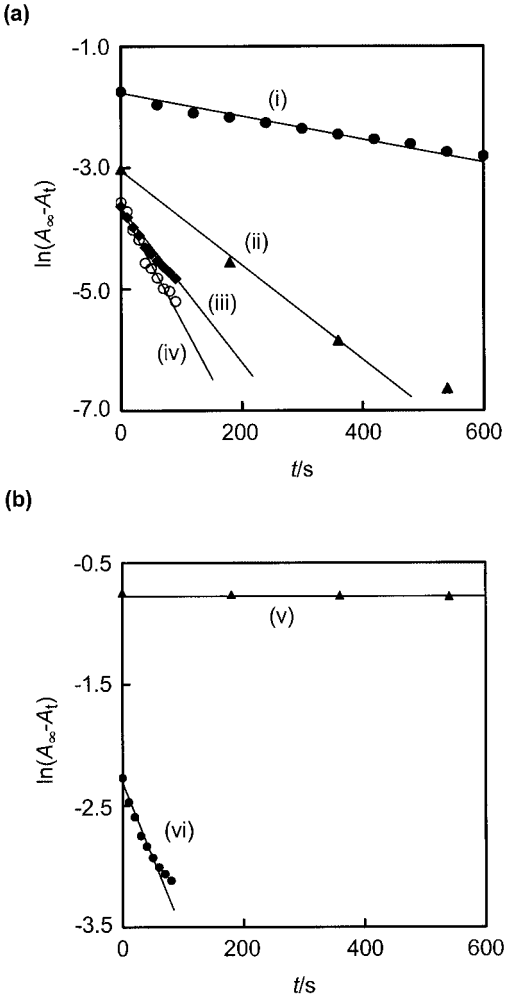

Figure 8. First-order plots of thermal isomerization (283 K) of (a) **4** in the photostationary state (i) without oxidation, (ii) after oxidation at 0.3 V, (iii) 0.6 V and (iv) 1.0 V, and (b) **5** in the photostationary state (iv) without oxidation and (v) after oxidation at 0.4 V; A_t denotes the absorption at 440 nm

Scheme 6 summarizes a mechanism that accounts for the rapid isomerization of the oxidized species. One-electron oxidation of **4** and **5**, with the azobenzene group *cis*, forms the Fe^{III} center, which is in equilibrium with the species having an Fe^{II} center and a cation radical at the N atom[16] due to electron transfer between the Fe and two N atoms.[7] This intermediate is responsible for the rapid isomerization of the *cis*-azobenzene to the *trans* form.[17] The positive charge at the N atom attached to the azobenzene unit enhances the isomerization of the N=N bond significantly due to rapid N−N bond rotation of the oxidized form. A canonical structure containing a diazaquionid moiety and a radical at an azobenzene nitrogen is involved in the oxidized species. Although the amount of the intermediate is small, rapid rotation of the N−N bond due to the single-bond

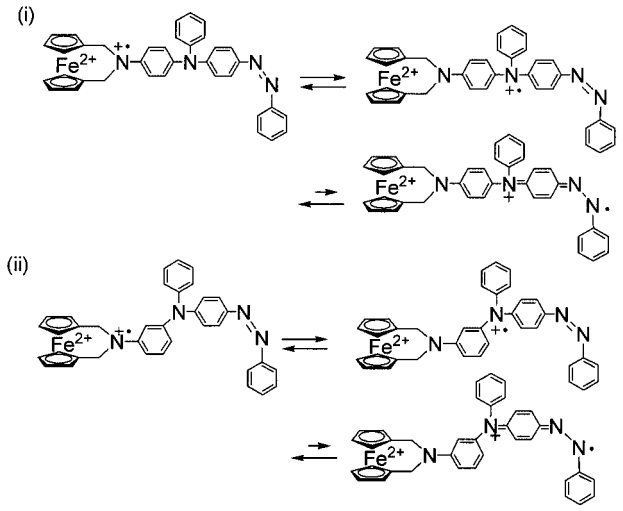

Scheme 6

character of the azobenzene group and intermolecular transfer of the positive charge at the organic ligand renders thermally induced isomerization facile.

In summary, the synthesis of new ferrocenophanes containing an azobenzene group has been achieved by using two types of bond-forming reactions catalyzed by transition metal complexes. The introduced azobenzene group performs as a redox-active site and as a chromophore that varies its absorption upon treatment with protic acid. The presence of ferrocenophane does not influence the optical properties of the azobenzene group significantly. Reversible multi-step redox reactions of **1** and **4** and the color change caused by addition of H^+ suggest a potential use of these compounds as electron- or acid-responsive organic materials.

Experimental Section

General Methods: $RuCl_2(PPh_3)_3$,[18] 1,1′-ferrocenedimethanol,[19] and $Pd_2(dba)_3$ [20] were prepared according to the literature. Preparation of the complexes and ferrocenophanes was carried out under nitrogen or argon using standard Schlenk techniques. Solvents were distilled from CaH_2 and stored under argon. The IR spectra were obtained with a JASCO-IR810 spectrophotometer. The ^1H and ^{13}C NMR spectra were recorded with a JEOL EX-400 spectrometer at 25 °C unless otherwise stated. A YANACO MT-5 CHN Autocorder was used for the elemental analyses. Cyclic voltammetry was recorded with a MeCN solution of 0.10 M Et_4NBF_4 with an ALS Electrochemical Analyzer Model-600A. The potentials were referenced to Ag^+/Ag. Spectroscopic measurements of the electrochemically oxidized species were carried out by using a combination of a flow-through electrolysis cell, ALS Electrochemical Analyzer Model-600A and EYELA peristaltic pump SMP-11, and JASCO V-530 UV/Vis spectrometer. Details of apparatus have been reported previously.[8,21]

Preparation of 1: 4-Phenylazoaniline (429 mg, 2.2 mmol) and then 1,1′-ferrocenedimethanol (536 mg, 2.2 mmol) were added at room temperature to a solution of $[RuCl_2(PPh_3)_3]$ (139 mg, 0.15 mmol) in 1-methyl-2-pyrrolidone (NMP) (3 mL) under nitrogen. The mixture was heated for 48 h at 180 °C. After removal of the solvent under vacuum, the product was extracted with ethyl acetate and purified by column chromatography (silica gel; hexane/ethyl acetate, 3:1). The yellow solid thus obtained was recrystallized from a dichloromethane/methanol mixture to afford **1** as orange crystals (253.0 mg, 38%). $C_{24}H_{21}FeN_3 \cdot 0.5C_6H_{14}$ (450.38): calcd. C 71.95, H 6.22, N 9.33; found C 72.11, H 6.07, N 9.33. ^1H NMR (400 MHz, $CDCl_3$, 25 °C): δ = 3.95 (s, 4 H, Cp-CH_2-N), 4.00, 4.15 (t, J = 2 Hz, 8 H, Cp), 6.95 (d, J = 10 Hz, 2 H, *meta*-N=NC$_6$H$_4$-), 7.37 (t, J = 7 Hz, 1 H, *para*-C$_6$H$_5$N=N-), 7.41 (t, J = 8 Hz, 2 H, *meta*-C$_6$H$_5$N=N-), 7.78 (d, J = 9 Hz, 2 H, *ortho*-N=NC$_6$H$_4$), 7.83 (d, J = 9 Hz, 2 H, *ortho*-C$_6$H$_5$N=N) ppm. $^{13}C\{^1H\}$ NMR (100 MHz, $CDCl_3$, 25 °C): δ = 45.8 (Cp-*C*H$_2$-N), 69.4 (Cp), 70.0, 83.4 (*Cp*-CH$_2$-), 112.0 (*para*-C$_6$H$_5$N=N-), 122.2 (*ortho*-C$_6$H$_5$N=N), 125.4 (*ortho*-C$_6$H$_4$N=N), 129.0 (*meta*-C$_6$H$_5$N=N-), 129.5 (*para*-C$_6$H$_5$N=N-), 144.2 (*ipso*-C$_6$H$_4$N=N), 151.1 (*para*-N=N C$_6$H$_4$-), 153.2 (*ipso*-C$_6$H$_5$N=N) ppm.

Preparation of 2: 4-Bromoaniline (571 mg, 3.3 mmol) and then 1,1′-ferrocenedimethanol (817 mg, 3.3 mmol) were added at room temperature to a solution of $[RuCl_2(PPh_3)_3]$ (139 mg, 0.15 mmol) in NMP (5 mL) under nitrogen. The mixture was heated for 24 h at 180 °C. After removal of the solvent under vacuum, the product was extracted with acetone. Column chromatography (silica gel; hexane/ethyl acetate, 1:1) of the extract gave a yellow solid which was recrystallized from a dichloromethane/methanol mixture to afford **2** as yellow crystals (883 mg, 70%). $C_{18}H_{16}BrFeN$ (382.08): calcd. C 56.58, H 4.22, Br 20.91, N 3.67; found C 56.85, H 4.06, Br 21.21, N 3.69. ^1H NMR (400 MHz, $CDCl_3$, 25 °C): δ = 3.84 (s, 4 H, Cp-CH_2-N), 4.06, (t, J = 2 Hz, 8 H, Cp), 6.83 (t, J = 9 Hz, 2 H, *meta*-BrC$_6$H$_4$), 7.32 (d, J = 9 Hz, 2 H, *ortho*-BrC$_6$H$_4$) ppm. $^{13}C\{^1H\}$ NMR (100 MHz, $CDCl_3$, 25 °C): δ = 46.1 (Cp-*C*H$_2$-N), 69.3, 70.0 (Cp), 84.0 (*Cp*-CH$_2$-), 113.1 (*ipso*-BrC$_6$H$_4$), 115.0 (*meta*-BrC$_6$H$_4$), 132.1 (*ortho*-BrC$_6$H$_4$), 148.3 (*para*-BrC$_6$H$_4$) ppm.

Preparation of 3: 3-Bromoaniline (571 mg, 3.3 mmol) and then 1,1′-ferrocenedimethanol (817 mg, 3.3 mmol) were added at room temperature to a solution of $[RuCl_2(PPh_3)_3]$ (139 mg, 0.15 mmol) in NMP (5 mL) under nitrogen. The mixture was heated for 24 h at 180 °C. After removal of the solvent under vacuum, the product was extracted with acetone. Column chromatography (silica gel; hexane/ethyl acetate, 1:1) of the extract gave a yellow solid which was recrystallized from a dichloromethane/methanol mixture to afford **3** as yellow crystals (857 mg, 68%). ^1H NMR (400 MHz, $CDCl_3$, 25 °C): δ = 3.84 (s, 4 H, Cp-CH_2-N), 4.06, 4.18 (t, J = 2 Hz, 8 H, Cp), 6.84 (d, J = 7 Hz, 1 H, *para*-BrC$_6$H$_4$), 6.85 (s, 1 H, *ortho*-BrC$_6$H$_4$), 7.08 (dd, J = 7 Hz, 1 H, *meta*-BrC$_6$H$_4$), 7.09 (d, J = 7 Hz, 1 H, *ortho*, BrC$_6$H$_4$) ppm. $^{13}C\{^1H\}$ NMR (100 MHz, $CDCl_3$, 25 °C): δ = 46.0 (Cp-*C*H$_2$-N), 69.3, 69.9 (Cp), 83.8 (*Cp*-CH$_2$-), 111.7 (*para*-BrC$_6$H$_4$), 115.9 (*ortho*-BrC$_6$H$_4$-N), 119.8 (*ortho*-BrC$_6$H$_4$), 123.7 (*ipso*-BrC$_6$H$_4$), 130.6 (*meta*-BrC$_6$H$_4$), 150.4 (*meta*-BrC$_6$H$_4$-N) ppm.

Preparation of 4: A mixture of **2** (382 mg, 1.0 mmol) and 4-phenylazodiphenylamine (273 mg, 1.0 mmol) was dissolved in toluene (20 mL). NaO*t*Bu (145 mg, 1.5 mmol), $Pd_2(dba)_3$ (12 mg, 0.013 mmol), and P(*t*Bu)$_3$ (15 mg, 0.075 mmol) were then added to the solution, which was stirred at 100 °C for 40 h under argon. After cooling, the reaction mixture was quenched by adding NH_4OH. The product was extracted with $CHCl_3$ and purified by column chromatography (silica gel; hexane/$CHCl_3$, 1:1) to give a red-orange solid. Recrystallization from a $CHCl_3$/hexane mixture gave **4** as red crystals (471 mg, 82%). $C_{36}H_{30}FeN_4$ (574.50): calcd. C 75.26, H 5.26, N 9.75; found C 74.99, H 5.17, N 9.71. ^1H NMR (400 MHz, $CDCl_3$, 25 °C): δ = 3.86 (s, 4 H, Cp-CH_2-N), 4.11, 4.22 (d, J = 2 Hz, 8 H, Cp), 6.95 (d, J = 9 Hz, 2 H, *meta*-CH$_2$NC$_6$H$_4$),

Table 2. Crystal data and details of structure refinement of **1**, **4**, and **5**

Compound	**1**	**4**	**5**
Formula	$C_{24}H_{21}FeN_3$	$C_{36}H_{30}FeN_4$	$C_{36}H_{30}FeN_4$
Molecular mass	407.30	574.50	574.50
Crystal system	monoclinic	monoclinic	triclinic
Space group	$P2_1/n$ (no. 14)	$P2_1$ (no. 4)	$P\bar{1}$ (no. 2)
a (Å)	13.186(2)	12.174(4)	10.362(2)
b (Å)	10.485(2)	10.819(3)	18.639(4)
c (Å)	15.008(3)	22.819(5)	7.399(2)
α (°)			97.97(2)
β (°)	113.59(1)	92.20(3)	102.67(2)
γ (°)			86.58(2)
V (Å^3)	1901.4(7)	2806(1)	1380.1(5)
Z	4	4	2
μ(Mo-K_α) (cm^{-1})	8.07	5.70	5.79
F(000)	848.00	1200.00	600.00
D_{calcd} (g cm^{-1})	1.423	1.360	1.382
Crystal size (mm)	0.2 × 0.4 × 0.4	0.8 × 0.8 × 1.0	0.4 × 0.5 × 0.7
Unique reflections	4613	6822	5105
Obsvd. reflections [$I \geq 3.0\sigma(I)$]	1438	2938	2381
No. of variables	253	738	370
R	0.043	0.046	0.047
R_w	0.038	0.054	0.033

7.09 (d, J = 7 or 9 Hz, 5 H, *ortho*-$CH_2NC_6H_4$, *ortho*- and *para*-NC_6H_5), 7.21 (d, J = 7 Hz, 2 H, *meta*-$C_6H_4N{=}N$), 7.31 (t, J = 7 Hz, 2 H, *meta*-C_6H_5N-), 7.41 (t, J = 7 Hz, 1 H, *para*-$C_6H_5N{=}N$-), 7.49 (t, J = 7 Hz, 2 H, *meta*-$C_6H_5N{=}N$-), 7.80 (d, J = 9 Hz, 2 H, *ortho*-$C_6H_4N{=}N$), 7.85 (d, J = 9 Hz, 2 H, *ortho*- $C_6H_5N{=}N$) ppm. $^{13}C\{^1H\}$ NMR (100 MHz, $CDCl_3$, 25 °C): δ = 45.8 (Cp-*C*H_2-N), 69.4 (Cp), 70.0, 83.4 (*Cp*-CH_2-), 115.1, 119.9, 122.4, 123.5, 124.2, 124.8, 128.1, 128.9, 129.3, 129.9, 136.7, 146.5, 147.0, 147.3, 151.1, 153.1 ppm.

Preparation of 5: A mixture of **3** (382 mg, 1.0 mmol) and 4-phenylazodiphenylamine (273 mg, 1.0 mmol) was dissolved in toluene (20 mL). NaO*t*Bu (145 mg, 1.5 mmol), $Pd_2(dba)_3$ (12 mg, 0.013 mmol), and P(*t*Bu)$_3$ (15 mg, 0.075 mmol) were then added to the solution, which was stirred at 100 °C for 40 h under argon. After cooling, the reaction mixture was quenched by adding NH_4OH. The product was extracted with $CHCl_3$ and purified by column chromatography (silica gel; hexane/$CHCl_3$, 1:1) to give a red-orange solid. Recrystallization from a $CHCl_3$/hexane mixture gave **5** as red crystals (448 mg, 78%). $C_{36}H_{30}FeN_4$ (574.50): calcd. C 75.26, H 5.26, N 9.75; found C 75.14, H 5.13, N 9.65. ^1H NMR (400 MHz, $CDCl_3$, 25 °C): δ = 3.81 (s, 4 H, Cp-C*H*$_2$-N), 4.07, 4.17 (d, J = 2 Hz, 8 H, Cp), 7.87−6.55 (aromatic protons) ppm. $^{13}C\{^1H\}$ NMR (100 MHz, $CDCl_3$, 25 °C): δ = 45.9 (Cp-*C*H_2-N), 69.2, 69.9 (Cp), 84.3 (*Cp*-CH_2-), 109.7, 111.1, 115.5, 121.3, 122.5, 123.9, 124.2, 125.4, 129.0, 129.4, 130.1, 130.4, 147.0, 148.2, 150.4, 150.7, 153.0 ppm.

X-ray Structure Analyses: Crystals of **1**, **4**, and **5** suitable for an X-ray diffraction study were obtained by recrystallization from CH_2Cl_2/MeOH and mounted in glass capillaries under argon. Data were collected at 23 °C on a Rigaku AFC-5R automated four-circle diffractometer equipped with monochromated Mo-K_α radiation (λ = 0.71073 Å). Calculations were carried out with the program package teXsan for Windows.[22] The structures were solved by direct methods and subsequent Fourier techniques. All non-hydrogen atoms were refined anisotropically. The hydrogen atoms were located by assuming an ideal geometry, and are included in the structure calculation without further refinement of the parameters. Crystallographic data and details of refinement are summarized in Table 2.

CCDC-242244 (for **1**), -213721 (for **4**), and -213722 (for **5**) contain the supplementary crystallographic data for this paper. These data can be obtained free of charge from The Cambridge Crystallographic Data Centre via www.ccdc.cam.ac.uk/data_request/cif.

Acknowledgments

This work was financially supported by the Shourai Foundation and a Grant-in-aid for Scientific Research for Priority Area (no. 15036223 "Dynamic Complexes") from the Ministry of Education, Culture, Sports, Science, and Technology Japan. M. H. acknowledges a Fellowship for Young Researchers from the Kitasato University Alumni Association.

[1] J. Chen, M. A. Reed, A. M. Rawlett, J. M. Tour, *Science* **1999**, *286*, 1550−1552.

[2] H. D. Sikes, J. F. Smalley, S. P. Dudek, A. R. Cook, M. D. Newton, C. E. Chidsey, S. W. Feldberg, *Science* **2001**, *291*, 1519−1523.

[3] [3a] D. M. Junge, D. V. McGrath, *J. Am. Chem. Soc.* **1999**, *121*, 4912−4913. [3b] A. M. Sanchez, M. Barra, R. H. de Rossi, *J. Org. Chem.* **1999**, *64*, 1604−1609. [3c] M. A. Lockwood, P. E. Fanwick, O. Einsenstein, I. P. Rothwell, *J. Am. Chem. Soc.* **1996**, *118*, 2762−2763. [3d] M. Ghedini, D. Pucci, A. Crispini, G. Barberio, *Organometallics* **1999**, *18*, 2116−2124.

[4] [4a] B. J. Coe, C. J. Jones, J. A. McCleverty, D. Bloon, P. V. Kolinsky, R. J. Jones, *J. Chem. Soc., Chem. Commun.* **1989**, 1485−1487. [4b] S.-M. Lee, M. Marcaccio, J. A. McCleverty, M. D. Ward, *Chem. Mater.* **1998**, *10*, 3272−3274. [4c] S. Barlow, H. E. Bunting, C. Ringham, J. C. Green, G. U. Bublitz, S. G. Boxer, J. W. Perry, S. R. Marder, *J. Am. Chem. Soc.* **1999**, *121*, 3715−3723. [4d] D. G. Walter, D. J. Compbell, C. A. Mirkin, *J. Phys. Chem. B* **1999**, *103*, 402−405. [4e] Y. Miyaki, T. Onishi, H. Kurosawa, *Chem. Lett.* **2000**, 1334−1335. [4f] M. Murata, M. Yamada, T. Fujita, K. Kojima, M. Kurihara, K. Kubo, Y. Kobayashi, H. Nishihara, *J. Am. Chem. Soc.* **2001**, *123*,

12903−12904. [4g] T. Muraoka, K. Kinbara, Y. Kobayashi, T. Aida, *J. Am. Chem. Soc.* **2003**, *125*, 5612−5613.
[5] [5a] M. Kurihara, K. Matsuda, A. Hirooka, T. Yutaka, H. Nishihara, *J. Am. Chem. Soc.* **2000**, *122*, 12373−12374. [5b] M. Kurihara, A. Hirooka, S. Kume, M. Sugimoto, H. Nishihara, *J. Am. Chem. Soc.* **2002**, *124*, 8800−8801.
[6] [6a] M. Horie, Y. Suzaki, K. Osakada, *J. Am. Chem. Soc.* **2004**, *126*, 3684−3685. [6b] H. Plenio, J. Yang, R. Diodone, J. Heinze, *Inorg. Chem.* **1994**, *33*, 4098−4104.
[7] [7a] I. Yamaguchi, T. Sakano, H. Ishii, K. Osakada, T. Yamamoto, *J. Organomet. Chem.* **1999**, *584*, 213−216. [7b] T. Sakano, H. Ishii, I. Yamaguchi, K. Osakada, T. Yamamoto, *Inorg. Chim. Acta* **1999**, *296*, 176−182. [7c] T. Sakano, K. Osakada, *Macromol. Chem. Phys.* **2001**, *202*, 1829−1836.
[8] T. Sakano, M. Horie, K. Osakada, H. Nakao, *Bull. Chem. Soc. Jpn.* **2001**, *74*, 2059−2065.
[9] M. Horie, T. Sakano, K. Osakada, H. Nakao, *Organometallics* **2004**, *23*, 18−20.
[10] [10a] S.-I. Murahashi, K. Kondo, T. Hakata, *Tetrahedron Lett.* **1982**, *23*, 229−232. [10b] Y. Watanabe, Y. Tsuji, H. Ige, Y. Ohsugi, T. Ohta, *J. Org. Chem.* **1984**, *49*, 3359−3363. [10c] Y. Tsuji, K.-T. Huh, Y. Ohsugi, Y. Watanabe, *J. Org. Chem.* **1985**, *50*, 1365−1370. [10d] Y. Tsuji, K.-T. Huh, Y. Yokoyama, Y. Watanabe, *J. Chem. Soc., Chem. Commun.* **1986**, 1575−1576. [10e] Y. Tsuji, Y. Yokoyama, K.-T. Huh, Y. Watanabe, *Bull. Chem. Soc. Jpn.* **1987**, *60*, 3456−3458.
[11] [11a] J. F. Hartwig, S. Richards, D. Barañano, F. Paul, *J. Am. Chem. Soc.* **1996**, *118*, 3626−3633. [11b] J. F. Hartwig, *Synlett* **1997**, 329−340. [11c] M. S. Driver, J. F. Hartwig, *J. Am. Chem. Soc.* **1997**, *119*, 8232−8245. [11d] L. M. Alcazar-Roman, J. F. Hartwig, A. L. Rheingold, L. M. Liable-Sands; I. A. Guzei, *J. Am. Chem. Soc.* **2000**, *122*, 4618−4630.
[12] [12a] A. S. Guram, R. A. Rennels, S. L. Buchwald, *Angew. Chem. Int. Ed. Engl.* **1995**, *34*, 1348−1350. [12b] J. P. Wolfe, S. Wagaw, S. L. Buchwald, *J. Am. Chem. Soc.* **1996**, *118*, 7215−7216. [12c] S. Wagaw, R. A. Rennels, S. L. Buchwald, *J. Am. Chem. Soc.* **1997**, *119*, 8451−8458. [12d] J.-F. Marcoux, S. Wagaw, S. L. Buchwald, *J. Org. Chem.* **1997**, *62*, 1568−1569. [12e] R. A. Singer, J. P. Sadighi, S. L. Buchwald, *J. Am. Chem. Soc.* **1998**, *120*, 213−214. [12f] D. W. Old, M. C. Harris, S. L. Buchwald, *Org. Lett.* **2000**, *2*, 1403−1406.
[13] [13a] N. P. Reddy, M. Tanaka, *Tetrahedron Lett.* **1997**, *38*, 4807−4810. [13b] M. Nishiyama, T. Yamamoto, Y. Koie, *Tetrahedron Lett.* **1998**, *39*, 617−620. [13c] M. Nishiyama, T. Yamamoto, Y. Koie, *Tetrahedron Lett.* **1998**, *39*, 2367−2370.
[14] [14a] J. D. Dunitz, L. E. Orgel, *Nature* **1953**, *171*, 121−122. [14b] N. D. Jones, R. E. Marsh, J. H. Richards, *Acta Crystallogr.* **1965**, *19*, 330−336. [14c] S.-J. Jong, J.-M. Fang, *Org. Lett.* **2000**, *2*, 1947−1949.
[15] [15a] R. Somoano, V. Hadek, S. P. S. Yen, A. Rembaum, *J. Chem. Phys.* **1975**, *62*, 1061−1067. [15b] J. Yamaguchi, H. Fujita, *Bull. Chem. Soc., Jpn.* **1990**, *63*, 2928−2932. [15c] A. G. MacDiarmid, J. C. Chiang, M. Halpern, W.-S. Huang, S.-B. Mu, N. L. D. Somasiri, W. Wu, S. Yaniger, *Mol. Cryst. Liq. Cryst.* **1985**, *125*, 173−176. [15d] H. Owano, H. Murakami, T. Yamashita, H. Ohigashi, *Synth. Met.* **1991**, *39*, 327−341. [15e] E. T. Kang, K. G. Neoh, K. L. Tan, *Prog. Polym. Sci.* **1988**, *23*, 277−324.
[16] [16a] M. R. Buchmeiser, N. Schuler, G. Kaltenhauser, K.-H. Ongania, I. Lagoja, K. Wurst, H. Schottenberger, *Macromolecules* **1998**, *31*, 3175−3183. [16b] M. R. Buchmeiser, *Macromolecules* **1998**, *31*, 3175−3183.
[17] [17a] A. Sanchez, R. H. de Rossi, *J. Org. Chem.* **1993**, *58*, 2094−2096. [17b] T. Enomoto, H. Hagiwara, D. A. Tryk, Z.-F. Liu, K. Hashimoto, A. Fujishima, *J. Phys. Chem. B* **1997**, *101*, 7422−7427.
[18] P. S. Hallman, T. A. Stephenson, G. Wilkinson, *Inorg. Synth.* **1970**, *12*, 237−240.
[19] A. S. Carlström, T. Frejd, *J. Org. Chem.* **1990**, *55*, 4175−4180.
[20] T. Ukai, H. Kawazura, Y. Ishii, J. J. Bonnet, J. A. Ibers, *J. Organomet. Chem.* **1974**, *65*, 253−266.
[21] [21a] T. Sakano, M. Horie, K. Osakada, H. Nakao, *Bull. Chem. Soc. Jpn.* **2001**, *74*, 2059−2065. [21b] H. Nakao, H. Hayashi, K. Okita, *Anal. Sci.* **2001**, *17*, 545−549.
[22] *CrystalStructure 3.6.0, Crystal analysis package*, Rigaku and Rigaku/MSC, **2000**−**2004**.

Received July 9, 2004
Published Online January 7, 2005

